*URSI AP-RASC 2019, New Delhi, India; 09 - 15 March 2019*

# Incorporation Algorithm with RPM and DBIM in Bayesian Framework for Microwave Non-destructive Testing

Shuto Takahashi*(1), Shouhei Kidera(1),(2)
(1) Graduate School of Informatics and Engineering,
University of Electro-Communications, Tokyo, Japan
(2) Japan Science Technology Agency, PRESTO, Saitama, Japan

## Abstract

Microwave non-destructive testing (NDT) is promising for non-contact and speedy survey for air cavity or metallic rust buried into concrete media in tunnel or highway. As an imaging algorithm for the above application, the distorted born iterative method (DBIM) is one of the promising options to retrieve not only target's location but its dielectric property, which is useful for material characterization. However, in an actual NDT scenario, scattered data from limited direction are available, which makes the problem more ill-posed. In this paper, the incorporation algorithm with radar approach as the range points migration (RPM) method, which offers a prior estimate of the region of interest (ROI), substantially reduces the number of unknowns in the DBIM. Furthermore, the variational Bayesian expectation maximization (VBEM) algorithm is introduced in the above incorporation. The finite-difference time-domain (FDTD) based numerical simulations demonstrate that the proposed method achieves faster convergence and more accurate results compared with that without the prior ROI estimation.

## 1 Introduction

Microwave non-destructive testing (NDT) techniques have a great attentions as speedy and large-scale non-contact screening technique for air crack or corrosion detection for aging transportation infrastructure *e.g.* tunnel or road, to avoid a voluntary collapse or catastrophe caused by an earthquake because it achieves a sufficient penetration depth and higher range resolution using ultra-wideband (UWB) pulse. Microwave NDT technique has some advantages from ultrasonic or hammering test because they are with contact measurement to avoid a large propagation loss in the air.

A number of microwave imaging techniques have been developed, which are categorized into two types. One is a confocal (radar) approach, which estimates targets shape and location based on the delay and sum (DAS) approach [1]. The other type is based on the inverse scattering analysis [2], which provides an estimate of dielectric profile by the inverse solution for the Helmholtz type domain integral equation, but it is non-linear and ill-posed nature in typical case. Furthermore, focusing on the NDT scenario, an omnidirectional observation, i.e., tomographic measurement, is hardly achieved, and it suffers from an extreme lack of data amount to get an accurate profile.

Recent studies [3] has revealed that various types of rust, *e.g.* black rust, salt rust or red rust, have different dielectric property, and the dielectric characterization is much important for recognizing whether metallic corrosion or air crack. According to this background, we focus on one of the most promising inverse scattering algorithm as the distorted born iterative method (DBIM) [2], which has been demonstrated that it retrieves high contrasted dielectric profile in various type of target or observation model. However, in the NDT model, the DBIM also suffers from the difficulty for a lack of data, and a large number of unknowns should be processed for large scale searching area, which incurs high computational cost and inaccuracy.

This paper incorporates radar imaging into the inverse scattering analysis to overcome the above-mentioned difficulty in the DBIM, in more particular manner, the region of interest (ROI) in the DBIM formulation is focused on the vicinity around object, which should be estimated by the radar imaging algorithm. As a promising radar imaging method, we introduce the range points migration (RPM) method, the effectiveness of which have been demonstrated in some literatures [4]. In particular, the literature [5] has verified that the RPM based method accomplishes the 1/100 wavelength order accuracy for buried object shape estimation in the NDT model. A prior estimate of the ROI by the RPM, the number of unknowns processed in DBIM are considerably downsized, which contributes to offer more accurate and rapid reconstruction of dielectric profile of targets, even in a seriously ill-posed situation. There are some options how to incorporate the prior ROI into the DBIM, and in this paper, we introduce the variational Bayesian expectation maximization (VBEM) algorithm [6] for it. The advantage for the use of VBEM is that it dynamically updates the ROI in each iterative step in the DBIM, and the hyper-parameters with respect to the ROI distribution is automatically determined by the EM algorithm. The finite-difference time-domain (FDTD) based numerical tests, assuming the typ-

ical NDT situation, where air cavity and some types of metallic rusts are buried into concrete media, demonstrates that the proposed method achieves faster and more accurate reconstruction compared with that by the DBIM without the ROI prior.

## 2 Observation Model and Data

Figure 1 shows the observation model. It assumes that a background media is homogeneous, low lossy, and non-dispersive dielectric media. A number of the transmitting and receiving antennae are arranged in front of background media. Note that, the relative permittivity and conductivity of background media are not given. The filter output (*e.g.* matched filter) at antenna location $\boldsymbol{r}$ is defined as $E(\boldsymbol{r},R)$, where $R = ct/2$ expressed by time $t$ and c is the speed of light in air. Range points extracted from local maxima of $E(\boldsymbol{r},R)$ as to $R$ are divided into two groups. one is defined as $\boldsymbol{q}_{1,i} \equiv (\boldsymbol{r}_{1,i}, R_{1,i})$ where each member having maximum $E(\boldsymbol{r},R)$ as to $R$. The remaining range points are categorized into $\boldsymbol{q}_{2,i} \equiv (\boldsymbol{r}_{2,i}, R_{2,i})$.

## 3 Method

### 3.1 Distorted Born Iterative method (DBIM)

A number of studies claimed that the DBIM is one of most promising approach for complex permittivity reconstruction, in biomedical or subsurface imaging applications. The forward scattering problem is described by the Helmholtz type domain integral as:

$$\begin{aligned}\Delta E^{\mathrm{t}}(\omega;\boldsymbol{r}_t,\boldsymbol{r}_r) &\equiv E^{\mathrm{t}}(\omega;\boldsymbol{r}_t,\boldsymbol{r}_r) - E^{\mathrm{t}}_{\mathrm{b}}(\omega;\boldsymbol{r}_t,\boldsymbol{r}_r) \\ &= \omega^2\mu \int_{\Omega} G_{\mathrm{b}}(\omega;\boldsymbol{r}_r,\boldsymbol{r}')E^{\mathrm{t}}(\omega;\boldsymbol{r}_t,\boldsymbol{r}')O(r')d\boldsymbol{r}'.\end{aligned} \tag{1}$$

where $E^{\mathrm{t}}(\omega;\boldsymbol{r}_t,\boldsymbol{r}_r)$ denotes the observed total field at antenna location $\boldsymbol{r}_r$ which is transmitted from $\boldsymbol{r}_t$, $E^{\mathrm{t}}_{\mathrm{b}}(\omega;\boldsymbol{r}_t,\boldsymbol{r}_r)$ is the total field in assuming the specific background media with complex permittivity $\varepsilon_{\mathrm{b}}(\boldsymbol{r})$, $G_{\mathrm{b}}(\omega;\boldsymbol{r}_r,\boldsymbol{r}')$ is the back ground Green's function, $\Omega$ is the region of interest (ROI). $O(\boldsymbol{r}) \equiv \varepsilon_r(\boldsymbol{r}) - \varepsilon_{\mathrm{b}}(\boldsymbol{r})$ is the object function where $\varepsilon_r(\boldsymbol{r})$ is complex permittivity of scatters. Under the Born's approximation, $E^{\mathrm{t}}(\omega;\boldsymbol{r}_t,\boldsymbol{r}') \simeq E^{\mathrm{t}}_{\mathrm{b}}(\omega;\boldsymbol{r}_t,\boldsymbol{r}')$ holds, and the following relationship is derived:

$$\Delta E^{\mathrm{t}}(\omega;\boldsymbol{r}_t,\boldsymbol{r}_r) \simeq \omega^2\mu \int_{\Omega} G_{\mathrm{b}}(\omega;\boldsymbol{r}_r,\boldsymbol{r}')E^{\mathrm{t}}_{\mathrm{b}}(\omega;\boldsymbol{r}_t,\boldsymbol{r}')O(r')d\boldsymbol{r}'. \tag{2}$$

The general DBIM algorithm iteratively updates $\varepsilon_{\mathrm{b}}(\boldsymbol{r})$, $G_{\mathrm{b}}(\omega;\boldsymbol{r}_r,\boldsymbol{r}')$ and $E^{\mathrm{t}}_{\mathrm{b}}(\omega;\boldsymbol{r}_t,\boldsymbol{r}')$ in order to minimize $\sum_{r_t,r_r} |\Delta E^{\mathrm{t}}(\omega;\boldsymbol{r}_t,\boldsymbol{r}_r)|^2$.

A lot of literature demonstrated that the DBIM offers accurate dielectric profiles even with high contrast object under various tomographic observation model, however, in most case of NDT scenario, a tomographic (omni-directional) observation is hardly achieved, namely, a limited directional data are available. Thus, it makes the problem more ill-posed, and extremely difficult to obtain a meaningful solution.

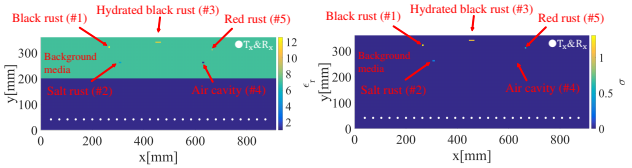


**Figure 1.** Observation model (a) relative permittivity and (b) conductivity

**Table 1.** Dielectric properties and size of background medium and each target.

| | $\varepsilon_r$ | $\sigma$ [S/m] | size [mm] |
|---|---|---|---|
| Background medium | 7.0 | 0.001 | $1006 \times 360$ |
| Black rust (#1) | 12.58 | 1.31 | $6 \times 6$ |
| Salt rust (#2) | 5.33 | 0.29 | $10 \times 6$ |
| Hydrated black rust (#3) | 11.28 | 1.14 | $22 \times 4$ |
| Air cavity (#4) | 1 | 0 | $8 \times 6$ |
| Red rust (#5) | 8.42 | 0.57 | $6 \times 6$ |

### 3.2 Incorporation with RPM and DBIM

To overcome the above difficulty, the incorporation with the RPM based ROI determination into the DBIM method is presented in this paper. The RPM converts a group of observed ranges to each corresponding scattering center by the Gaussian kernel estimator. The details of the RPM method is described in [4]. Assuming the actual scenario, a dielectric property of background media is roughly estimated by the DBIM by assuming that a whole ROI is homogeneous. Then, the RPM determines each scattering center corresponding to range point $\boldsymbol{q}_{2,i}$ assuming homogeneous media with the estimated relative permittivity of the background media.

The RPM image is formed as an aggregation of scattering center points, then, we should consider how to implement the RPM image into the ROI (finite area) in the DBIM framework. Here, we consider two types of implementation approaches, one is based on fixed ROI, and the other is dynamical ROI determination based on Bayesian framework.

#### 3.2.1 CGLS based optimization

In this case, for each scattering center point, the small size of ROI is given as $\Omega_i^{\mathrm{obj}}$, where $i$ denotes the index of scattering center. The DBIM reconstructs the dielectric profile by (2). The optimization is done by the CGLS algorithm, where the ROI, namely $\Omega_i^{\mathrm{obj}}$ is fixed through the optimization process.

#### 3.2.2 VBEM based optimization

The previous approach is based on the fixed ROI in the iterative process in DBIM, and thus, the accuracy of the DBIM

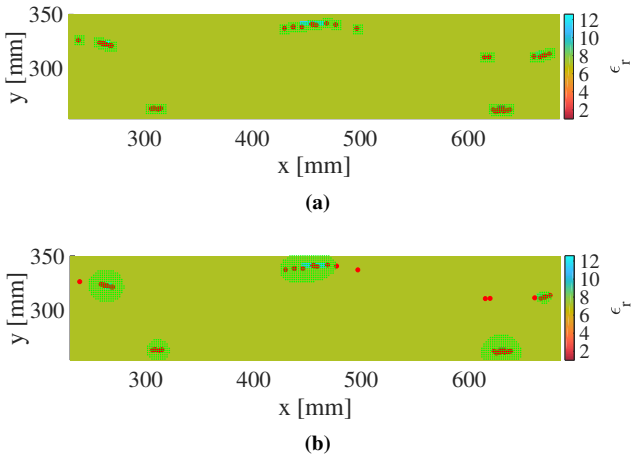


**Figure 2.** ROI (green dots) limited by the RPM imaging points (red solid circles), (a) fixed ROI case, (b) variant ROI case.

significantly depends on the initial estimate of the ROI. To avoid such initial value dependency, another approach is introduced so that the ROI is updated in the iterative process in DBIM. As a suitable approach for this purpose, we focus on the Bayesian framework, where the ROI is given as the prior distribution. Let the following conditional probability density function (PDF) about the total field $\boldsymbol{E}$ and the object function $\boldsymbol{O}$ as normal distributions:

$$p(\boldsymbol{E}|B\boldsymbol{O},\beta) = \mathcal{N}(\boldsymbol{E}|\boldsymbol{B}\boldsymbol{O},\beta^{-1}\boldsymbol{I}), \tag{3}$$

$$p(\boldsymbol{O}|\boldsymbol{\alpha}) = \prod_{i=1}^{N} \mathcal{N}(O_i|0,{\alpha_i}^{-1}), \tag{4}$$

where $N$ is total number of unknowns in $\Omega$, $\boldsymbol{E},\boldsymbol{B}$ and $\boldsymbol{O}$ are discritized version of $\Delta E^{\mathrm{t}}(\omega;\boldsymbol{r}_t,\boldsymbol{r}_r), \omega^2\mu G_{\mathrm{b}}(\omega;\boldsymbol{r}_r,\boldsymbol{r}')E^{\mathrm{t}}_{\mathrm{b}}(\omega;\boldsymbol{r}_t,\boldsymbol{r}')$ and $\boldsymbol{O}(\boldsymbol{r}')$, $\beta$ and $\boldsymbol{\alpha} \equiv [\alpha_1,\ldots,\alpha_N]$ are the precision parameters (hyper parameters) in each normal distribution. Here, the PDF of $\boldsymbol{\alpha}$ is defined using the Gamma priors as:

$$p(\boldsymbol{\alpha}) = \prod_{i=1}^{N} \mathrm{Gamma}(\alpha_i|a_i,b_i) = \prod_{i=1}^{N} \frac{b_i^{a_i}}{\Gamma(a_i)} \alpha_i^{a_i-1} e^{-b_i\alpha_i}, \tag{5}$$

where $\mathrm{Gamma}(x|a,b)$ is the gamma distribution with the parameters $a$ and $b$. The maximum a posteriori (MAP) estimates is formulated as

$$\hat{\boldsymbol{O}} = \arg\max_{\boldsymbol{O}} p(\boldsymbol{O}|\boldsymbol{\alpha}). \tag{6}$$

To solve the above optimization problem, the VBEM algorithm iteratively updates $\bar{\boldsymbol{O}}$ as:

$$\bar{\boldsymbol{O}} = \beta(\bar{\boldsymbol{A}} + \beta\boldsymbol{B}^T\boldsymbol{B})^{-1}\boldsymbol{B}^T\boldsymbol{E}, \tag{7}$$

$$\tag{8}$$

where

$$\bar{\boldsymbol{A}} = \mathrm{diag}(\bar{\boldsymbol{\alpha}}), \tag{9}$$

$$\bar{\alpha}_i = \frac{a_i + \frac{1}{2}}{b_i + \frac{1}{2}({\bar{O}_i}^2 + S_{i,i})}, \tag{10}$$

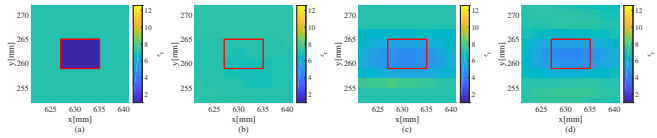

**Figure 3.** Reconstructed relative permittivity for air cavity (#4), (a) Original profile, (b) Original DBIM, (c) Proposed method with CGLS, (d) Proposed method with VBEM (red line: true ROI boundary).

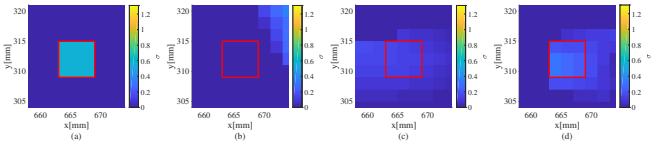

**Figure 4.** Reconstructed conductivity for red rust (#5), (a) Original profile, (b) Original DBIM, (c) Proposed method with CGLS, (d) Proposed method with VBEM (red line: true ROI boundary).

$\bar{\boldsymbol{\alpha}} \equiv [\bar{\alpha_1},\ldots,\bar{\alpha_N}]$, and $S_{i,i}$ is $i$-th diagonal element of $\boldsymbol{S}$.

In this framework, it is well-known fact that the region with large $\bar{\boldsymbol{\alpha}}$ is regarded as low probability area of target existing. Focusing on this fact, initial value of $\bar{\alpha}_i$ is given by the following equation exploiting the RPM results:

$$\bar{\alpha}_i = \left\{ \sum_{m=1}^{N^{\mathrm{rpm}}} F_m \mathcal{N}(\boldsymbol{r}^i|\hat{\boldsymbol{p}}(\boldsymbol{q}_{2,m}),\boldsymbol{S}_r) \right\}^{-1}, \tag{11}$$

where $\boldsymbol{r}^i$ is $i$-th cell in ROI, $\boldsymbol{S}_r$ is diagonal matrix which determines the intensity of $\alpha_i$ around ecah scatterig point, $\hat{\boldsymbol{p}}(\boldsymbol{q}_{2,m}), m = 1,\ldots,N^{\mathrm{rpm}}$ is the estimated scattering points by RPM, and $F_m$ is given by

$$F_m = \sum_{j,k} g(\boldsymbol{q}_{2,m};\boldsymbol{q}_{2,j},\boldsymbol{q}_{2,k}) \times \exp\left\{ -\frac{\|\boldsymbol{p}^{\mathrm{int}}_{m,j,k} - \hat{\boldsymbol{p}}(\boldsymbol{q}_{2,m})\|^2}{\sigma_r^2} \right\}. \tag{12}$$

where $g(\boldsymbol{q}_{2,m};\boldsymbol{q}_{2,j},\boldsymbol{q}_{2,k})$ is the weighting function [4], $\boldsymbol{p}^{\mathrm{int}}_{i,j,k}$ is the intersection point among the three orbits of propagation paths and $\sigma_r$ is a constant. In each DBIM iterative sequences, $\bar{\boldsymbol{\alpha}}$, that is, the ROI is updated.

## 4 Numerical Test

This section describes the two-dimensional (2-D) FDTD based numerical simulation to test the performance of each method. The NDT observation model illustrated in Fig. 1 is assumed. 27 set of transmitting and receiving antenna are linearly arranged with 30 mm equally spacing, the location of which is 158 mm far from the concrete surface. The transmitted signal is formed Gaussian-modulated pulse with 2.45 GHz center frequency and 2.7 GHz bandwidth. Five different types of targets, as air cavity and different types of metallic rusts, are buried into concrete media. Each target size and its dielectric property is summarized in Table 1, where the dielectric property of rust is referred from [3]. The cell size of both the forward (FDTD)

**Table 2.** The estimated mean relative permittivity and conductivity $(\varepsilon_r, \sigma)$ of each target for each method.

| | Original | DBIM | DBIM w RPM (CGLS) | DBIM w RPM (VBEM) |
|---|---|---|---|---|
| #1 | (12.58, 1.31) | (7.20, 0.46) | (7.55, 0.28) | (7.58, 0.27) |
| #2 | (5.33, 0.29) | (7.08, 0.07) | (6.44, 0.10) | (6.65, 0.10) |
| #3 | (11.28, 1.14) | (7.32, 0.22) | (7.30, 0.39) | (7.04, 0.47) |
| #4 | (1, 0) | (6.99, 0.35) | (4.89, 0.00) | (4.85, 0.01) |
| #5 | (8.42, 0.57) | (7.13, 0.00) | (7.18, 0.13) | (7.60, 0.24) |

and inverse (DBIM) solutions is 2 mm square. The total number of unknowns including the concrete (background) media is 40240.

As to the initial estimation of the background property determined by the DBIM, we obtained the estimations of relative permittivity is 7.1547 and the conductivity is 0.0021 S/m. Figure 2 shows the scattering center points estimated by the RPM, in two different algorithms for ROI determinations described as in Sec. 3.3.1 and Sec. 3.3.2. Here, the CGLS based algorithm, the ROI for each scattering center is determined as the region spanned by $5 \times 5$ cells, and is fixed through the DBIM iteration. In the VBEM based algorithm, the ROI is determined by using Eq. (11). The number of unknowns for the original DBIM, the proposed method with CGLS and that with VBEM are 80480, 960 (98.8 % reduced) and 1782 (97.8 % reduced), respectively. Figures 3 and 4 show the reconstructed dielectric maps for air cavity and red rust, by the original DBIM method, where the whole ROI area is processed, the proposed method with CGLS, and that with VBEM. These figures clearly shows that the proposed method enhances reconstruction accuracy compared with the original DBIM. Furthermore, Fig. 3 and 4 show that the VBEM based algorithm achieves more accurate reconstruction with respect to both dielectric property and target's shape compared with the CGLS based algorithm.

For quantitative analysis of each method, Table 2 shows the estimated mean relative permittivity and conductivity of each target. This result demonstrate that the proposed method incorporating the RPM and DBIM significantly enhances the reconstruction accuracy. Furthermore, Fig. 5 shows the residual of cost functions as $\sum_{r_t,r_r} |\Delta E^{\mathrm{t}}(\omega; \boldsymbol{r}_t, \boldsymbol{r}_r)|^2$ for each iteration number. This results also shows the VBEM based algorithm achieves faster convergence, because this algorithm exploits prior information about unknowns in ROI given by RPM and updates ROI in each DBIM iteration.

## 5 Conclusion

This paper proposed an efficient inverse scattering algorithm by incorporating the RPM into the DBIM for the microwave NDT via VBEM based Bayesian approach. To achieve the above incorporation, the RPM results are exploited as a prior estimate of the ROI in the DBIM, which contributes a remarkable reduce of a number of unknown in DGIM. In addition, the two types of the ROI implementation based on CGLS and VBEM are presented, where the

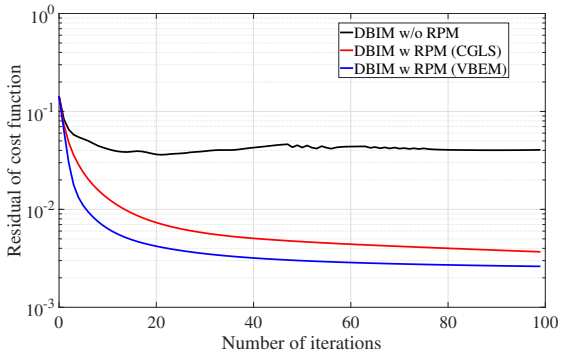


**Figure 5.** The residual of cost functions as $\sum_{r_t,r_r} |\Delta E^{\mathrm{t}}(\omega; \boldsymbol{r}_t, \boldsymbol{r}_r)|^2$ for each iteration number.

VBEM enables us to update the ROI in the DBIM iterative sequences. The FDTD-based numerical simulations, assuming NDT observation model, demonstrated that the ROI determination by RPM improved reconstruction accuracy, even for the extremely ill-posed scenario, and expands the application range of the inverse scattering analysis.

## 6 Acknowledgements

This research was supported by JST, PRESTO, Grant Number JPMJPR1771, Japan.

## References

[1] M. Fallahpour, J.T. Case, M. Ghasr, and R. Zoughi, " Piecewise and wiener filter-based sar techniques for monostatic microwave imaging of layered structures", *IEEE Trans. Antennas Propaga*, vol. 62, no. 1, pp. 1-13, Jan. 2014

[2] W. C. Chew and Y. M. Wang, " Reconstruction of two-dimensional permittivity distribution using the distorted Born iterative method, " *IEEE Trans. Med. Imag.*, vol. 9, pp. 218-225, June 1990.

[3] R. Zoughi, *Microwave Nondestructive Testing and Evaluation*, The Netherlands: Kluwer Academic, 2000.

[4] K. Akune, S. Kidera, and T. Kirimoto "Accurate and Nonparametric Imaging Algorithm for Targets Buried in Dielectric Medium for UWB Radars," *IEICE Trans.* Electronics., vol. E95-C, No. 8, pp. 1389-139, Aug. 2012.

[5] T. Manaka, S. Kidera and T. Kirimoto, " Experimental study on embedded object imaging method with range point suppression of Creeping Wave for UWB radars ", *IEICE Trans. Electron* Vol.E99-C,No.1,pp.138-142, Jan. 2016.

[6] L. Gharsalli, H. Ayasso, B. Duchene, and A. M. Djafari, " Inverse scattering in a Bayesian framework: Application to microwave imaging for breast cancer detection, " *Inv. Prob.*, vol. 30, no. 11, pp. 1-26, 2014.